

INTEGRO-DIFFERENTIAL EQUATIONS FOR ANTI-PLANE
CRACKS IN INHOMOGENEOUS PIEZOELECTRIC PLANE

Marin Marinov, Tsviatko Rangelov*

(Submitted by Academician P. Popivanov on July 19, 2011)

Abstract

Anti-plane cracks in functionally graded piezoelectric plane under time-harmonic loads are studied by boundary integral equation method (BIEM). Exponential variation of the material parameters is considered. The numerical solution provides crack opening displacement from which the generalized intensity factor (GIF) is determined. Numerical examples demonstrate the dependence of GIF on inhomogeneity parameters and on dynamic load.

Key words: functionally graded piezoelectric solid, anti-plane cracks, BIEM, GIF

2000 Mathematics Subject Classification: 74E05, 74F15, 74S15, 74H35

1. Introduction. The importance of the investigation of functionally graded piezoelectric materials (FGPM) is due to their application in transducers, actuators, wave generators and other smart intelligent systems. During the manufacturing process and also in service conditions cracks and other defects that cause failure of these devices can appear.

There are mainly two semi-analytical numerical methods for studying of the elastodynamic problems in inhomogeneous domains. One of them is the dual integral equation method, see [3, 4, 9, 10, 14], where anti-plane line cracks in domains

The authors acknowledge the support of the Bulgarian National Science Fund under Grant No. DID 02/15.

with exponentially varying properties in parallel or perpendicular direction to the crack line are studied. The boundary value problem (BVP) is transformed to dual integral equations on the crack line and GIF is obtained as a solution of a suitable Fredholm integral equation.

Another method is the boundary integral equation method (BIEM), treated in [5,6,13] where arbitrary shaped anti-plane cracks in domains with quadratic, sinusoidal or exponential inhomogeneity are investigated. The BVP is transformed to an equivalent integro-differential equation (IDE) on the crack and crack opening displacement (COD) is found using BIEM. In this case the solution can be obtained in every point of the domain together with the GIF – the leading coefficient in the asymptotic of the solution near the crack edges.

The aim of the work is to solve an IDE for anti-plane cracked FGPM with exponentially varying properties. The fundamental solution obtained by using the Radon transform is implemented in the created by Mathematica software numerical code. The applicability of the presented BIEM is demonstrated by numerical examples.

2. Statement of the problem. We consider a piezoelectric plane with an arbitrary shaped finite crack $\Gamma = \Gamma^+ \cup \Gamma^-$ – an open arc, poled in x_3 direction and subjected to time-harmonic loading.

The mechanical and electrical loading is assumed to be such that the only unvanishing displacements are the anti-plane mechanical displacement $u_3(x, t)$ and the in-plane electrical displacements $D_i = D_i(x, t)$, $i = 1, 2$, $x = (x_1, x_2)$. Since all fields are time-harmonic with the frequency ω the common multiplier $e^{i\omega t}$ is suppressed here and in the following. For such a case, assuming quasi-static approximation of piezoelectricity, the field equation in absence of body force is given by the balance equation

$$(1) \quad \sigma_{i3,i} + \rho\omega^2 u_3 = 0, \quad D_{i,i} = 0,$$

the strain–displacement and electric field–potential relations

$$(2) \quad s_{i3} = u_{3,i}, \quad E_i = -\Phi_{,i},$$

and the constitutive relations, see [8]

$$(3) \quad \begin{aligned} \sigma_{i3} &= c_{44}s_{i3} - e_{15}E_i, \\ D_i &= e_{15}s_{i3} + \varepsilon_{11}E_i. \end{aligned}$$

The subscript $i = 1, 2$ and comma denotes partial differentiation. Here σ_{i3} , s_{i3} , E_i , Φ are the stress tensor, strain tensor, electric field vector and electric potential respectively. Furthermore, $\rho(x) > 0$, $c_{44}(x) > 0$, $\varepsilon_{11}(x) > 0$ are the inhomogeneous mass density, the shear stiffness, piezoelectric and dielectric permittivity

characteristics. Introducing (3) and (2) into (1) leads to the coupled system

$$(4) \quad \begin{aligned} (c_{44}u_{3,i})_{,i} + (e_{15}\Phi_{,i})_{,i} + \rho\omega^2u_3 &= 0, \\ (e_{15}u_{3,i})_{,i} - (\varepsilon_{11}\Phi_{,i})_{,i} &= 0, \end{aligned}$$

where the summation convention over repeated indices is applied. The basic equations can be written in a more compact form if the notation $u_J = (u_3, \Phi)$, $J = 3, 4$ is introduced. The constitutive equations (3) then take the form

$$(5) \quad \sigma_{iJ} = C_{iJKl}u_{K,l}, \quad i, l = 1, 2,$$

where $C_{i33l} = \begin{cases} c_{44}, & i = l \\ 0, & i \neq l \end{cases}$, $C_{i34l} = C_{i43l} = \begin{cases} e_{15}, & i = l \\ 0, & i \neq l \end{cases}$, $C_{i44l} = \begin{cases} -\varepsilon_{11}, & i = l \\ 0, & i \neq l \end{cases}$ and equation (4) is reduced to

$$(6) \quad \sigma_{iJ,i} + \rho_{JK}\omega^2u_K = 0, \quad J, K = 3, 4,$$

where $\rho_{JK} = \begin{cases} \rho, & J = K = 3 \\ 0, & J = 4 \text{ or } K = 4. \end{cases}$

Along the crack line it is supposed

$$(7) \quad t_J = 0 \quad \text{on } \Gamma,$$

where $t_J = \sigma_{iJ}n_i$ and $n = (n_1, n_2)$ is the outer normal vector to Γ^+ . The boundary condition (7) means that the crack faces are free of mechanical traction as well as of surface charge, i.e. the crack is electrically impermeable.

We further assume that the mass density and material parameters vary in the same manner with x , through function $h(x) = e^{2\langle a, x \rangle}$, where $\langle \cdot, \cdot \rangle$ means the scalar product in R^2 , and $a = (a_1, a_2)$, such that

$$(8) \quad c_{44}(x) = c_{44}^0h(x), \quad e_{15}(x) = e_{15}^0h(x), \quad \varepsilon_{11}(x) = \varepsilon_{11}^0h(x), \quad \rho(x) = \rho^0h(x).$$

One way to solve the problem (6), (7) numerically is to transform it into the equivalent integro-differential equation along the crack Γ . This can be done if we are able to use an appropriate fundamental solution for equation (6).

3. Fundamental solution and free field solution. 3.1. Fundamental solution. The fundamental solution of equation (6) is defined as solution of equation

$$(9) \quad \sigma_{iJM,i}^* + \rho_{JK}\omega^2u_{KM}^* = -\delta_{JM}\delta(x, \xi),$$

where $\sigma_{iJK}^* = C_{iJML}u_{KM,l}^*$, $J, K, M = 3, 4$, $i, l = 1, 2$, δ is the Dirac function, $x = (x_1, x_2)$, $\xi = (\xi_1, \xi_2)$ and δ_{JM} is the Kronecker symbol. For the considered

inhomogeneity function $h(x)$ the fundamental solution is obtained in [12] as follows. First equation (9) is transformed by a suitable change of functions to an equation with constant coefficients. In a second step we apply Radon transform which allows the construction of a set of fundamental solutions depending on the roots of the characteristic equation of the obtained ODE-system. Finally, using both the inverse Radon transform and the inverse change of functions, the fundamental solutions of equation (6) is obtained in a closed form. In the first step the smooth transformation $u_{KM}^* = h^{-1/2}U_{KM}^*$ applied to (9) gives

$$(10) \quad C_{iJKi}^0 U_{KM,ii}^* + [\rho_{JK}^0 \omega^2 - C_{iJKi}^0 a_i^2] U_{KM}^* = h^{-1/2}(\xi) \delta_{JM} \delta(x, \xi).$$

To solve equation (10) we use the Radon transform, see ZAYED [18]. In R^2 it is defined for $f \in \mathfrak{S}$ the set of rapidly decreasing C^∞ functions as, $\hat{f}(s, m) = R[f(x)] = \int_{\langle m, x \rangle = s} f(x) dx = \int f(x) \delta(s - \langle m, x \rangle) dx$ with the inverse transform $f(x) = \frac{1}{4\pi^2} \int_{|m|=1} K(\hat{f}(s, m))|_{s=\langle m, x \rangle} dm$, $K(\hat{f}) = \int_{-\infty}^{\infty} \frac{\partial_\sigma \hat{f}(\sigma, m)}{s - \sigma} d\sigma$. Applying the Radon transform to both sides of (10), we get with $p_{JK} = C_{iJKi}^0 a_i^2$

$$(11) \quad [C_{iJKi}^0 m_i^2 \partial_s^2 + (\rho_{JK}^0 \omega^2 - p_{JK})] \hat{U}_{KM}^* = -h^{-1/2}(\xi) \delta_{JM} \delta(s - \langle \xi, m \rangle).$$

These two systems of two linear second order ordinary differential equations are solved following [15]. Denote $\gamma = (\rho^0 \omega^2 - a_0 p) a_0^{-1}$, $a_0 = c_{44}^0 + \frac{e_{15}^{02}}{\varepsilon_{11}^0}$, $\omega_0 = \sqrt{\frac{a_0}{\rho^0}} |a|$. Due to the frequency ω we obtain the solutions of (11) as follows:

(i) for $\gamma > 0$, i.e. $\omega > \omega_0$, $k = \sqrt{\gamma}$,

$$(12) \quad \begin{aligned} \hat{U}_{33}^* &= h^{-1/2}(\xi) \frac{i}{2ka_0} e^{ik|s-\tau|}, \quad \hat{U}_{34}^* = h^{-1/2}(\xi) \frac{i}{2ka_0} \frac{e_{15}^0}{\varepsilon_{11}^0} e^{ik|s-\tau|} \\ \hat{U}_{43}^* &= \hat{U}_{34}^*, \quad \hat{U}_{44}^* = h^{-1/2}(\xi) \left[\frac{i}{2ka_0} \left(\frac{e_{15}^0}{\varepsilon_{11}^0} \right)^2 e^{ik|s-\tau|} + \frac{1}{\varepsilon_{11}^0} \frac{1}{2|a|} e^{|a||s-\tau|} \right]; \end{aligned}$$

(ii) for $\gamma = 0$, i.e. $\omega = \omega_0$

$$(13) \quad \begin{aligned} \hat{U}_{33}^* &= -h^{-1/2}(\xi) \frac{1}{2a_0} |s - \tau|, \quad \hat{U}_{34}^* = -h^{-1/2}(\xi) \frac{1}{2a_0} \frac{e_{15}^0}{\varepsilon_{11}^0} |s - \tau| \\ \hat{U}_{43}^* &= \hat{U}_{34}^*, \quad \hat{U}_{44}^* = \frac{h^{-1/2}(\xi)}{2|a|} \left(\frac{1}{\varepsilon_{11}^0} - \frac{e_{15}^0}{a_0 \varepsilon_{11}^0} + \frac{e_{15}^{02}}{a_0 \varepsilon_{11}^0} \right) e^{|a||s-\tau|} \\ &\quad - h^{-1/2}(\xi) \left[\frac{1}{2a_0} \left(\frac{e_{15}^0}{\varepsilon_{11}^0} \right)^2 |s - \tau| \right]. \end{aligned}$$

(iii) for $\gamma < 0$, i.e. $\omega < \omega_0$, $k = \sqrt{|\gamma|}$,

$$(14) \quad \begin{aligned} \hat{U}_{33}^* &= -h^{-1/2}(\xi) \frac{1}{2ka_0} e^{k|s-\tau|}, \quad \hat{U}_{34}^* = -h^{-1/2}(\xi) \frac{1}{2ka_0} \frac{\epsilon_{15}^0}{\epsilon_{11}^0} e^{k|s-\tau|} \\ \hat{U}_{43}^* &= \hat{U}_{34}^*, \quad \hat{U}_{44}^* = -h^{-1/2}(\xi) \left[\frac{1}{2ka_0} \left(\frac{\epsilon_{15}^0}{\epsilon_{11}^0} \right)^2 e^{k|s-\tau|} - \frac{1}{\epsilon_{11}^0} \frac{1}{2|a|} e^{|a||s-\tau|} \right]. \end{aligned}$$

In order to obtain the fundamental solution we finally have to apply inverse Radon transform to \hat{U}_{KJ}^* . Since the functions \hat{U}_{KJ}^* are linear combinations of $e^{iq|s-\tau|}$, $e^{q|s-\tau|}$ and $|s-\tau|$, for the first part of the inverse Radon transform the formulas

$$(15) \quad \begin{aligned} K(e^{iq|s-\tau|}) &= -iq\{i\pi e^{iq\beta} - 2[\text{ci}(q\beta) \cos(q\beta) + \text{si}(q\beta) \sin(q\beta)]\}_{|\beta=|s-\tau|}, \\ K(e^{q|s-\tau|}) &= q\{2[\text{chi}(q\beta) \cosh(q\beta) - \text{shi}(q\beta) \sinh(q\beta)]\}_{|\beta=|s-\tau|}, \\ K(|s-\tau|) &= 2 \ln |\beta|_{|\beta=|s-\tau|}, \end{aligned}$$

are used where $\text{ci}(\eta) = -\int_{\eta}^{\infty} \frac{\cos t}{t} dt$, $\text{si}(\eta) = -\int_{\eta}^{\infty} \frac{\sin t}{t} dt$ are the cosine integral and sine integral functions and $\text{chi}(\eta) = -\int_0^{\eta} \frac{\cosh t - 1}{t} dt + \ln \eta + C$, $\text{shi}(\eta) = -\int_0^{\eta} \frac{\sinh t}{t} dt$ are the hyperbolic cosine and sine integral functions with Euler's constant C , see BATEMAN and ERDELYI [2].

After having obtained \hat{U}_{KJ}^* by completing inverse Radon transforms the final form of the fundamental solution is derived from the smooth transformation.

3.2. Free field solution. We are asking for a solution of Eq. (6) of the form

$$(16) \quad \begin{aligned} u(x, \eta) &= h^{-1/2}(x) U(x, \eta) = h^{-1/2} p e^{ik \langle x, \eta \rangle}, \\ p &= (p_1, p_2), \eta = (\eta_1, \eta_2), |\eta| = 1, \end{aligned}$$

where p is a polarization vector, k is a wave number and η is a direction of the incident wave. Again there are three cases with respect to ω .

(i) $\omega > \omega_0$. In this case $k = \pm \sqrt{\frac{\rho^0 \omega^2}{a_0} - |a|^2}$, the corresponding polarization vector is $p = \left(1, \frac{\epsilon_{15}^0}{\epsilon_{11}^0} \right)$ and

$$(17) \quad \begin{aligned} u(x, \eta) &= \begin{pmatrix} 1 \\ \frac{\epsilon_{15}^0}{\epsilon_{11}^0} \end{pmatrix} e^{\langle ik\eta - a, x \rangle} \\ t_3(x, \eta)|_{\Gamma^+} &= a_0 \langle ik\eta - a, n \rangle e^{\langle a + ik\eta, x \rangle}, \quad t_4(x, \eta)|_{\Gamma^+} = 0. \end{aligned}$$

(ii) $\omega = \omega_0$. In this case $k = 0$, the corresponding polarization vector is $p = \left(1, \frac{e_{15}^0}{\varepsilon_{11}^0}\right)$ and

$$(18) \quad u(x, \eta) = e^{-\langle a, x \rangle} \begin{pmatrix} 1 \\ \frac{e_{15}^0}{\varepsilon_{11}^0} \end{pmatrix}$$

$$t_3(x, \eta)|_{\Gamma^+} = -a_0 \langle a, n \rangle e^{\langle a, x \rangle}, t_4(x, \eta)|_{\Gamma^+} = 0.$$

(iii) $\omega < \omega_0$. In this case $k = \pm i \sqrt{\left|\frac{\rho^0 \omega^2}{a_0} - |a|^2\right|}$, the corresponding polarization vector is $p = \left(1, \frac{e_{15}^0}{\varepsilon_{11}^0}\right)$ and

$$(19) \quad u(x, \eta) = e^{-\langle a, x \rangle} \begin{pmatrix} 1 \\ \frac{e_{15}^0}{\varepsilon_{11}^0} \end{pmatrix} e^{\langle |k|\eta - a, x \rangle}$$

$$t_3(x, \eta)|_{\Gamma^+} = a_0 \langle |k|\eta - a, n \rangle e^{\langle a + |k|\eta, x \rangle}, t_4(x, \eta)|_{\Gamma^+} = 0.$$

4. Non-hypersingular BIEM. The non-hypersingular traction based BIE is derived following the procedure given in [7] and [17]. Using superposition principle the displacements and the traction are represented as $u_J = u_J^{in} + u_J^{sc}$, $t_J = t_J^{in} + t_J^{sc}$ where u_J^{in} , t_J^{in} is the free field solution and its traction on Γ (see section 3). From the boundary condition (7) we have $t_J^{sc} = -t_J^{in}$ on Γ . Let us introduce the smooth change of functions

$$(20) \quad u_J(x, \omega) = e^{-\langle a, x \rangle} W_J(x, \omega)$$

and suppose that $W_J(x, \omega)$ satisfies Sommerfeld-type condition on infinity, more specifically

$$(21) \quad W_3 = o(|x|^{-1}), W_4 = o(e^{-|a||x|}) \quad \text{for } |x| \rightarrow \infty.$$

Condition (21) ensures uniqueness of the scattering field u_J^{sc} for a given incident field u_J^{in} . Following AKAMATSU and NAKAMURA [1] it can be proved that the boundary value problem (BVP) (6), (7) admits continuous differentiable solutions.

For u_J, u_{JK}^* we apply the Green formula in the domain $\Omega_R \setminus \Omega_\varepsilon$, Ω_R is a disk with large radius R and Ω_ε is a small neighbourhood of Γ . Applying the representation formulae for the generalized displacement gradient $u_{K,l}$, see [17], an integro-differential equation on $\partial\Omega_R \cup \partial\Omega_\varepsilon$ is obtained. Using condition (20) integrals over $\partial\Omega_R$ go to 0 for $R \rightarrow \infty$. Taking the limit $\varepsilon \rightarrow 0$, i.e. $x \rightarrow \Gamma$ and

using the boundary condition (7), i.e. $t_J^{sc} = -t_J^{in}$ on Γ the following system of BIE is equivalent to the BVP (6), (7)

$$(22) \quad \begin{aligned} -t_J^{in}(x) = C_{iJKl}n_i(x) \int_{\Gamma^+} [(\sigma_{\eta PK}^*(x,y)\Delta u_{P,\eta}(y) \\ -\rho_{QP}\omega^2 u_{QK}^*(x,y)\Delta u_P(y))\delta_{\lambda l} - \sigma_{\lambda PK}^*(x,y)\Delta u_{P,l}(y)]n_\lambda(y)d\Gamma, \quad x \in \Gamma. \end{aligned}$$

Here, u_{JK}^* is the fundamental solution of (9), derived in Section 3, $\sigma_{iJQ}^* = C_{iJKl}u_{KQ,l}^*$ is the corresponding stress, and $\Delta u_J = u_J|_{\Gamma^+} - u_J|_{\Gamma^-}$ is the generalized COD. Equation (22) constitutes a system of integro-differential equations for the unknown Δu_J on the crack line Γ . From its solution the generalized displacement u_J at every internal point of the plane can be determined by using the corresponding representation formulae, see [13].

5. Numerical realization and results. 5.1. Numerical realization.

The numerical procedure for the solution of the boundary value problem follows the numerical algorithm developed and validated in [7, 11, 13]. The crack Γ is discretized by quadratic boundary elements (BE) away from the crack-tips and special crack-tip quarter-point BE near the crack-tips to model the asymptotic behaviour of the displacement and the traction. Applying the shifted point scheme, the singular integrals converge in Cauchy principal value (CPV) sense, since the smoothness requirements $\Delta u_J \in C^{1+\alpha}(\Gamma)$ of the approximation are fulfilled. Due to the form of the fundamental solution as an integral over the unit circle, all integrals in Eq. (22) are two dimensional. The regular integrals are solved using Monte Carlo method, while the singular integrals are solved with a combined method – partially analytically as CPV integrals.

After the discretization procedure an algebraic linear complex system of equations is obtained and solved. The programme code based on Mathematica has been created following the above outlined procedure.

The mechanical dynamic SIF K_{III} , the electrical displacement intensity factor K_D and the electric field intensity factor K_E are obtained directly from the traction nodal values ahead of the crack-tip. For example, in case of a straight crack, the interval $(-c, c)$ on the Ox_1 axis, the expressions are

$$(23) \quad \begin{aligned} K_{III} &= \lim_{x_1 \rightarrow \pm c} t_3 \sqrt{2\pi(x_1 \mp c)}, \quad K_D = \lim_{x_1 \rightarrow \pm c} t_4 \sqrt{2\pi(x_1 \mp c)}, \\ K_E &= \lim_{x_1 \rightarrow \pm c} E_3 \sqrt{2\pi(x_1 \mp c)}, \quad E_3 = \frac{e_{15}}{e_{15}^2 + c_{44}\epsilon_{11}}(-e_{15}t_3 + c_{44}t_4), \end{aligned}$$

where t_J is the generalized traction at the point $(x_1, 0)$ close to the crack-tip.

The Mathematica's code consists of the following parts: (i) Definition of the material parameters, crack geometry, BE and quadratic approximation; (ii) Definition of the fundamental solution, its derivatives and the asymptotic for small arguments; (iii) Definition of the integro-differential equations and the anti-plane

load; (iv) Solution of the integrals and forming the system of linear equations for the unknowns COD; (v) Solution of the linear system; (vi) Formulae for the solution in every point of the plane; (vii) Evaluation of the SIF – the leading coefficients in the asymptotic of the solution near the crack edges.

The main points in the solution procedure are (iv) and (v). In (iv) the integrals over the BE are two-dimensional (in the intrinsic coordinates in the domain $(z, \varphi) \in [-1, 1] \times [0, 2\pi]$) with regular and singular kernels: with weak singularity as $O(\log|x|)$ and with strong singularities $O(1/|x|)$. The regular integrals are solved using AdaptiveMonteCarlo Method with 300 points. The singular integrals are solved analytically with respect to r and numerically with respect to φ , and due to their oscillatory behaviour they are treated as 0.5 by two dimensional integral and solved again with AdaptiveMonteCarlo Method. The difficulties in (v) (due to the fact that the material parameters vary in the rate of 10^{10} : for mechanical stiffness c_{44} , 10 for the piezoelectric parameter e_{15} and for the dielectric parameters ε_{11} in the rate of 10^{-10}) are got over using functions Solve or FindInstance. The existing analytical solution in [16] for the homogeneous case FGPM helps for the validation of the BIEM solution.

5.2. Numerical results. The material used in the numerical examples is PZT-4, which data are $c_{44}^0 = 2.56 \times 10^{10}$ N/m², $e_{15}^0 = 12.7$ C/m², $\varepsilon_{11}^0 = 64.6 \times 10^{-10}$ C/Vm and $\rho^0 = 7.5 \times 10^3$ kg/m³. The crack half-length is $c = 5$ mm, it lies on the interval $(-c, c) \subset Ox_1$ and is discretized by 5 BE. In the figures, the absolute value of the normalized GIF $K_{III}^* = \frac{K_{III}}{\tau\sqrt{\pi c}}$, $K_E^* = \frac{K_E}{\tau\sqrt{\pi c}}$, $\tau = t_3^{in}$ is plotted versus the normalized frequency $\Omega = c\sqrt{\rho^0/a_0}\omega$.

The validation study is presented in [11] for the homogeneous PEM. The inhomogeneity parameter r is set to 0 and the BIEM result is compared with the result in [16]. It is noted that the maximum difference between both results obtained by different methods is about 7% – 10%.

In Figure 1 is given the BIEM solution for $rc = 0.4$, $\alpha = \pi/2$ and $\alpha = 0$ for normal incident wave. In this case the critical value of the normalized frequency is $\Omega_0 = 0.4$ where a jump of the GIF K_{III}^* and K_E^* appears. For $\Omega_0 > \Omega$ the dynamic behaviour is simple vibration, while for $\Omega_0 < \Omega$ the dynamic behaviour is a wave propagation and the curve is similar to the homogeneous case. Also for $\alpha = 0$ the GIF at the left crack-tip is higher then at the right crack-tip, while for $\alpha = \pi/2$ the value of the GIF in both crack-tips is equal.

In Figure 2 *a, b* for $rc = 0.4$ and the normal incident wave, the dependance of the GIF on $\alpha = m\frac{\pi}{10}$, $m = 1, \dots, 9$ for fixed normalized frequency $\Omega = 1.0$ is shown.

The numerical examples show the dependence on the magnitude r and on the direction α of the material inhomogeneity as well as the different behaviour of the GIF with respect to the critical value Ω_0 of the normalized frequency.

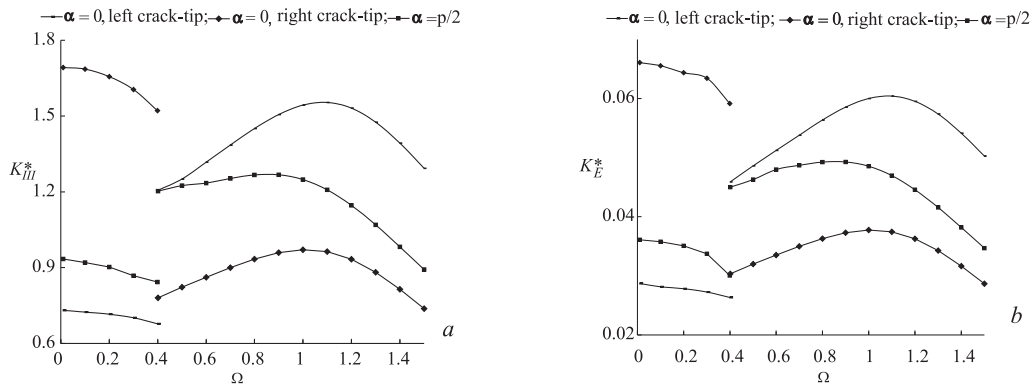


Fig. 1. Normalized GIF versus Ω for $rc = 0.4$ and $\alpha = 0, \alpha = \pi/2$: a) K_{III}^* ; b) K_E^*

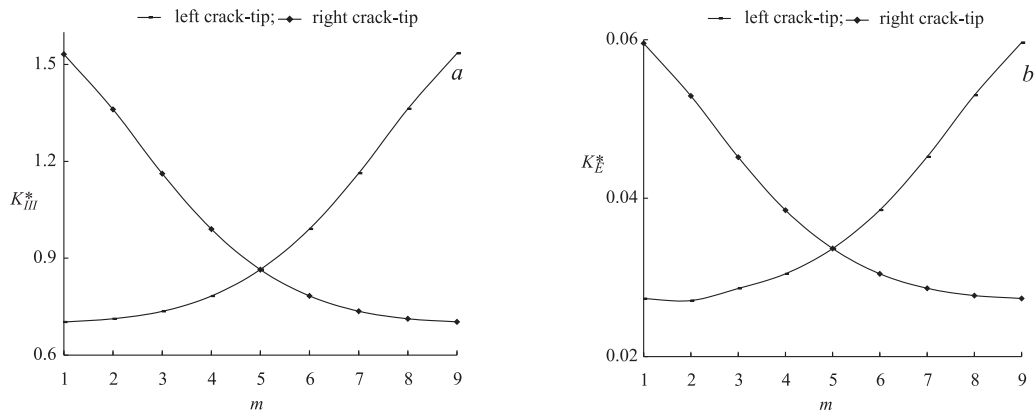


Fig. 2. Normalized GIF for fixed $\Omega = 1.0$, $rc = 0.4$ and $\alpha = m\frac{\pi}{10}$, $m = 1, \dots, 9$: a) K_{III}^* ; b) K_E^*

6. Conclusions. It is presented a numerical solution of integro-differential equations for anti-plane cracked FGPM. Using the derived with Radon transform fundamental solutions an efficient BIEM and a Mathematica programme code is developed. Numerical examples for SIF computation are presented. The proposed methodology, numerical solution and programme code can be applied for problems in non-destructive material testing as well as for solution of inverse problems in finite solids.

REFERENCES

- [1] AKAMATSU M., G. NAKAMURA. Appl. Anal., **81**, 2002, 129–141.
- [2] BATEMAN H., A. ERDELYI. Higher Transcendental Functions, New York, McGraw-Hill, 1953.

- [3] CHEN J., ZH. LIU, ZH. ZOU. *Int. J. Fracture*, **121**, 2003, 81–94.
- [4] CHAN Y. S., G. H. PAULINO, A. C. FANNJIANG. *Int. J. Solids Struct.*, **38**, 2001, 2989–3005.
- [5] DAROS C. H. *ZAMM-Z. Angew. Math. Mech.*, **90**, 2010, 113–121.
- [6] DINEVA P., D. GROSS, R. MÜLLER, T. RANGELOV. *Int. J. Solids Struct.*, **47**, 2010, 3150–3165.
- [7] GROSS D., T. RANGELOV, P. DINEVA. *J. Structural Integrity Durability*, **1**, 2005, No 1, 35–47.
- [8] LANDAU L. D., E. M. LIFSHITZ. *Electrodynamics of Continuous Media*, Oxford, Pergamon Press, 1960.
- [9] LI C., G. WENG. *J. Appl. Mech. (ASME)*, **69**, 2002, 481–488.
- [10] MA L., L. Z. WU, Z. G. ZHOU, L. C. GUO, L. P. SHI. *Eur. J. Mech. A/Solid*, **23**, 2004, 633–643.
- [11] MARINOV M., T. RANGELOV. In: *Proceedings of the 6 ICCSE 2010* (eds R. Stainov, V. Kanabar, P. Assenova), Germany, Fulda, 2010, 158–167.
- [12] RANGELOV T., P. DINEVA. *Compt. rend. Acad. bulg. Sci.*, **60**, 2007, No 3, 231–238.
- [13] RANGELOV T., P. DINEVA, D. GROSS. *ZAMM-Z. Angew. Math. Mech.*, **88**, 2008, 86–99.
- [14] SINGH B. M., R. S. DHALIWAL, J. VRBIK. *Proc. R. Soc., A* **465**, 2009, 1249–1269.
- [15] VLADIMIROV V. *Equations of mathematical physics*, Moscow, Nauka, 1984.
- [16] WANG X. D., S. A. MEGUID. *Mech. Mater.*, **32**, 2000, 723–737.
- [17] WANG C.-Y., CH. ZHANG. *Eng. Anal. Bound. Elem.*, **29**, 2005, 454–465.
- [18] ZAYED A. *Handbook of Generalized Function Transformations*, Boca Raton, Florida, CRC Press, 1996.

*Computer Science Department
New Bulgarian University
1618 Sofia, Bulgaria
e-mail: mlmarinov@nbu.bg*

**Institute of Mathematics and Informatics
Bulgarian Academy of Sciences
Acad. G. Bonchev Str., Bl. 8
1113 Sofia, Bulgaria,
e-mail: rangelov@math.bas.bg*